Front. Agr. Sci. Eng. 2018, **5**(2): 168–176
https://doi.org/10.15302/J-FASE-2018217
Available online at http://journal.hep.com.cn/fase

RESEARCH ARTICLE

Three-dimensional numerical simulation of flow in trapezoidal cutthroat flumes based on FLOW-3D

Danjie RAN, Wene WANG (✉), Xiaotao HU

Key Laboratory of Agricultural Soil and Water Engineering in Arid and Semiarid Areas of the Ministry of Education, Northwest A&F University, Yangling 712100, China

Abstract To solve the common problem of flumes flow-measurement accuracy without sacrificing water head, a new type of trapezoidal cutthroat flume to measure the discharge in terminal trapezoidal channels is presented. Using the computational fluid dynamic method, three-dimensional flow fields in trapezoidal cutthroat flumes were simulated using the RNG k-ε three-dimensional turbulence model along with the TruVOF technique. Simulations were performed for 12 working conditions, with discharges up to 0.075 $m^3 \cdot s^{-1}$ to determine hydraulic performance. Experimental data for the trapezoidal cutthroat flume in terminal trapezoidal channel were also obtained to validate the simulation results. Velocity distribution of the flume obtained from simulation analyses were compared with observed results based on time-averaged flow field and comparison yielded a solid agreement between results from the two methods, with relative error below 10%. The results indicated that the Froude number and the longitudinal average velocity increased along the convergence section and decreased in the divergent section. In the upper throat, the Froude number was less than 0.5, which meets the water measurement requirement, and the critical flow appeared near the throat section. The maximum water head loss of the trapezoidal cutthroat flume was less than 9% of the total head, compared to the rectangular cutthroat flume, and head loss of trapezoidal cutthroat flume was significantly less. Regression models developed for upstream depth versus discharge under different working conditions were satisfactory, with a relative error of less than 2.06%, which meets the common requirements of flow measurement in irrigation areas. It was concluded that trapezoidal cutthroat flumes can improve flow-measurement accuracy without sacrificing water head.

Keywords distribution of velocity, Froude number, head loss, stage-discharge relationship, trapezoidal cutthroat flume

1 Introduction

Nowadays, water crises are more and more seriously, and irrigated agriculture consumes more than 70% of the available water resources in the world[1]. Despite an extreme lack of water, there is often a tremendous waste of water used in agriculture. Due to rapid socio-economic development and continuing population growth, in future irrigated agriculture will face greater challenges in order to meet the growing food demand, while the water available for agriculture will simultaneously be decreasing[2]. Therefore, optimal allocation of water availability for agricultural irrigation in an efficient manner is a critical issue for agricultural water management[3]. Many irrigation areas use open channels to transfer water from headwaters to the field. Usually, the rate of flow along the channel, i.e., the discharge, must be known. Accurate discharge measurement is an important parameter in the management of irrigation systems and has a highly significant influence on the allocation of the irrigation water and strengthens the water-saving consciousness of water users. Wang[4] concluded that flumes, compared to other existing flow-measuring devices, are more suitable for flow measurement in open channels and are easier to apply.

Many investigators have studied the flow characteristics when measuring flumes. In the eighteenth century, Venturi was the first to observe the effect of a local contraction in a conduit on the pressure and velocity distribution[5]. Consequently, Venturi channels[6] were proposed and widely applied. Parshall[7] developed an improved Venturi flume; a simpler, less expensive and more accurate flume, which became known as the Parshall flume. In 1967, Skogerboe and Hyatt[8] proposed a rectangular cutthroat flume, which consisted of converging sections and diverging sections with no throat between them. Long-throated flumes have been accepted as the standard for

Received July 9, 2017; accepted November 24, 2017

Correspondence: wangwene@nwsuaf.edu.cn

flow measurement over recent decades[9]. Trapezoidal channels have been widely used for important irrigation and drainage channels in China because they have better hydraulic characteristics than rectangular channels and are easier to construct and maintain than U-shaped channels[10]. However, there is no discharge measurement structure highly suited to trapezoidal channels. Parshall flumes[11,12] and rectangular cutthroat flumes[8] are widely used in various channels[12–15] because of their advantages, such as no silting and high accuracy. However, the use of these discharge measurement structures results in large head loss and construction difficulty when used in trapezoidal channels because they do not have a trapezoidal cross section. To overcome these limitations, we proposed a trapezoidal cutthroat flume specifically designed for trapezoidal channels. In the past, the water measurement facilities were studied by model test. In recent years, however, numerical simulation of computational fluid dynamics has been widely used in the study of flumes. Computational fluid dynamics technology makes up for the deficiency of theoretical analysis and test and has the advantages of low cost, short time, relative ease of obtaining data in the flow field and for flow field visualization. In this study, a series of flume tests was performed under different discharge conditions with particular emphasis on the effect of structural parameters, using appropriate structural parameters for trapezoidal cutthroat flumes deduced theoretically. These parameters were then evaluated by laboratory experiments and FLOW-3D software.

2 Physical model and experimental setup

2.1 Physical model

Trapezoidal cutthroat flumes can be used under free and submerged flow conditions. The converging section, the trapezoidal throat and the diverging channel bottom section, were placed at suitable positions in the trapezoidal channel for practical application and divided into 14 measuring cross sections in laboratory experiments to measure hydraulic flow parameters. The throat of the flume must have a contraction ratio which ensures the occurrence of the critical flow condition. The trapezoidal cutthroat flume contraction ratio is defined as the area ratio of the throat section to the approach channel section. Figure 1 is a schematic of trapezoidal cutthroat flume. The flume contraction ratio was 0.506. The flume was 1.80 m long and 0.5 m high, with the base of the trapezoidal throat 0.18 m wide and side walls at 75° to the bottom of the flume.

2.2 Experimental setup and procedure

The trapezoidal cutthroat flume was constructed at the Fluvial Hydraulics Laboratory of Northwest A&F University, Yangling, China. The flume was installed in a trapezoidal channel. Figure 2 shows the experimental system, which consists of a reservoir, a pumping station, an electromagnetic flowmeter, a regulating valve, a stabilization pond, water supply pipes, trapezoidal channel, trapezoidal cutthroat flume, a tailgate, an outlet pound, a water return pipe and a 90° V-notch weir. The base slope of the concrete trapezoidal channel is 1/2000, the slope coefficient m = 1, the base width B = 0.30 m, the canal height H = 0.50 m, the channel length is 34 m, and the channel integrated rough coefficient n = 0.013. The flume was placed at a suitable position in the trapezoidal channel, making sure the centerline of the throat section form work coincided with the center line of the approach channel. There was an appropriate distance between the cross section of the water inlet in the channel and the entrance to the flume, so water in front of the flume entrance flowed smoothly. This setup was similar to actual working conditions.

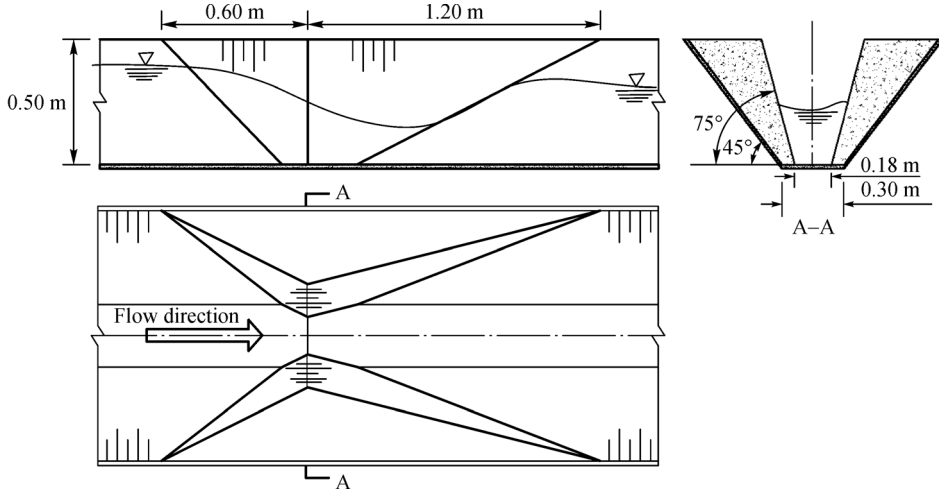

Fig. 1 Schematic of trapezoidal cutthroat flume

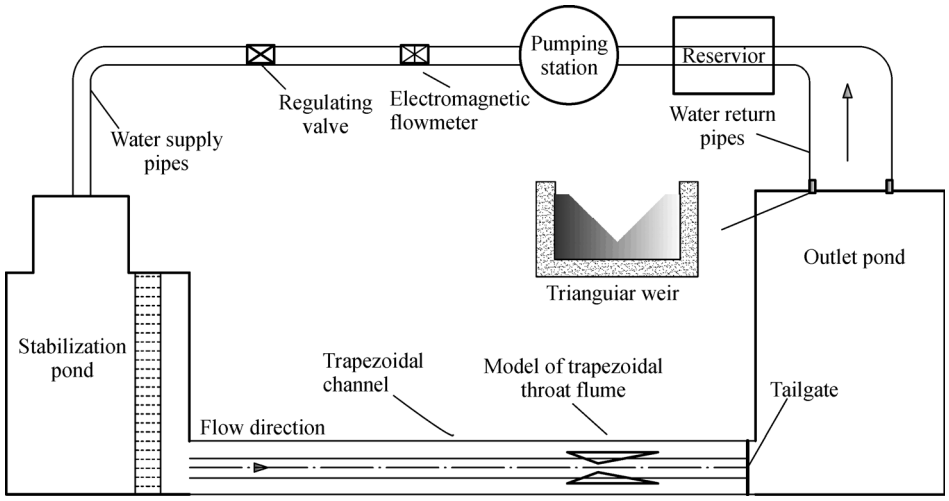

Fig. 2 Experimental layout for testing a trapezoidal cutthroat flume for measurement accuracy

The actual discharges in experiments were measured by a 90° V-notch weir using empirical Eq. (1)[10]. Depths of cross sections were recorded by a point gauge with resolution of 0.1 mm. Twelve laboratory experiments under free and submerged flow conditions were conducted for evaluating the hydraulic performance of trapezoidal cutthroat flumes. Water pumped into the flume flowed through the flume and then entered the backwater drainage channel. Once the flow stabilized, discharges were measured by the 90° V-notch weir, and the depths of each flume cross section were recorded.

$$Q = 1.343H^{2.47} \times 1000 \quad (1)$$

where Q is the discharge through the flume and H is the water head over the triangular weir.

3 Mathematical models and numerical methods

3.1 Governing equations and turbulence model

Numerical simulations were performed with the (computational fluid dynamics) FLOW-3D software[16,17]. The flow measurement of trapezoidal cutthroat flumes in trapezoidal channels is incompressible and viscous fluid motion. According to the basic law of physical conservation, the flow of flume is a Newton fluid. And In this case, the flow is described by the continuity and Navier-Stokes relationship. To consider the impact of pulsation, the time averaging method is widely used. The control equations of the flow of turbulence are given by Eqs. (2)–(4).

$$\frac{\partial \rho}{\partial t} + \frac{\partial(\rho u_i)}{\partial x_i} = 0 \quad (2)$$

$$\frac{\partial(\rho\mu_i)}{\partial t} + \frac{\partial(\rho\mu_i\mu_j)}{\partial x_j} = \frac{\partial}{\partial x_j}\left(\mu\frac{\partial \mu_i}{\partial x_j} - \rho\overline{\mu_i'\,\mu_j'}\right) - \frac{\partial p}{\partial x_i} + S_i \quad (3)$$

$$\frac{\partial(\rho\phi)}{\partial t} + \frac{\partial(\rho\mu_j\phi)}{\partial x_j} = \frac{\partial}{\partial x_j}\left(\Gamma\frac{\partial \phi}{\partial x_j} - \rho\overline{\mu_i'\,\mu_j'}\right) + S \quad (4)$$

where ρ is density of the fluid, t is flow time, u_i and u_j are represent average flow velocity components in Cartesian coordinates x, y and z, respectively ($\mathrm{m\cdot s^{-1}}$) (i = 1,2,3; j = 1,2,3), μ is the dynamics viscosity of fluid, p is the pressure and S_i is the source term, $S_1 = 0$, $S_2 = 0$, $S_3 = -\rho g$ (N).

The finite difference method was adopted to solve the governing equations with a second-order upwind scheme. TruVOF[18–21] was used to simulate the flow fields in the trapezoidal cutthroat flume. Employing the TruVOF method, empty cells are given a value of zero, full cells are given a value of one, and cells that contain the free surface are given a value representing the ratio of the fluid volume to cell volume. The water surface is then described as a first-order approximation according to the fluid-to-cell volume ratio and the location of the fluid in the surrounding cells. Using the TruVOF method, FLOW-3D can track free surfaces in both time and space. Only the value for the fluid was computed, not the value for the air. This method was used to reduce the time and describe the shape of the free surface graphically. When the standard k-ε model is used for the strong swirl flow or the flow with the wall surface, there will be some distortion. For this reason, Yakhot and Orzag propose the RNG k-ε model, which has the following main changes:

(1) By modifying the turbulent viscosity, the rotation and rotational flow in average flow are considered;

(2) Added an additional term in the ε equation, which reflects the mainstream of the mean strain rate and is not

only related to the movement, but also is a function of spatial coordinates in the unified problem.

Therefore, the RNG k-ε model can better deal with the high strain rate and the greater curvature of streamline flow.

In the study of airfoil flume simulation, Pan et al.[22], using the realizable k-ε, standard k-ε and RNG k-ε turbulence model, and compared with the experimental results, showing that the modified RNG k-ε turbulence model can deal with the channel flow measurements best. To allow the closure of the Navier-Stokes equations, the RNG k-ε model was used to account for turbulence and possible hydraulic jumps (Eqs. (5)–(6))[22]. TruVOF calculation method can accurately track the change of free liquid surface and accurately simulate the flow problem with free interface. The equation is given by Eq. (7)[23].

$$\frac{\partial(\rho k)}{\partial t}+\frac{\partial(\rho k u_i)}{\partial x_i}=\frac{\partial}{\partial x_j}\left[\alpha_k \mu_{eff}\frac{\partial k}{\partial x_j}\right]+G_k+\rho\varepsilon \tag{5}$$

$$\frac{\partial(\rho\varepsilon)}{\partial t}+\frac{\partial(\rho\varepsilon u_i)}{\partial x_i}=\frac{\partial}{\partial x_j}\left[\alpha_\varepsilon \mu_{eff}\frac{\partial \varepsilon}{\partial x_j}\right]+\frac{C_{1\varepsilon}^{*}\varepsilon}{k}G_k+C_{2\varepsilon}\rho\frac{\varepsilon^2}{k} \tag{6}$$

where k is the turbulence kinetic energy, u_i is mean velocity, G_k is generation item produced by the turbulence kinetic energy, $C_{1\varepsilon}$ and $C_{2\varepsilon}$ are empirical constants, whose values are 1.42 and 1.68, respectively, ε is the turbulence dissipation rate.

$$\frac{\partial(F)}{\partial t}+\underline{u}_m\cdot\nabla F=0 \tag{7}$$

where $\underline{u}_m$ is the average velocity of the mixture, t is time, F is the volume fraction of the fluid required.

3.2 Description of the model and mesh generation

The dimensions and flow conditions of the numerical model were the same as the laboratory model above. The three-dimensional geometries of the numerical model were created using Pro/Engineer 5.0[24,25]. Meshes were established for flow domain by the FAVOR[26–29] (fractional area volume obstacle representation) method that generates grids. Appropriate mesh structure and size are important for the accuracy and convergence of numerical solutions. In this case, the size of the grid was set to 0.02 m long, 0.02 m wide and 0.02 m high, and the number of all the grids was 783000. Employing the FAVOR method, grids generating the model used the finite difference method to simulate complicated models. Furthermore, the FAVOR method used fewer hexahedron grid units than the established methods which, in terms of the proportion of the flow domain, smooths and eliminates the rough regions, and therefore builds a mesh model without any distortion.

3.3 Computational method and boundary conditions

The boundary conditions of the numerical model in this work are presented in Fig. 3. The flow from the inlet to the outlet of the channel was open to the atmosphere. The inlet boundary was a specified volumetric flow rate from the whole open area of the channel inlet on the upstream side, with auto-adjusted fluid height. The flow rate of inlet is set according to the corresponding experimental flow conditions. The flume was placed at a suitable position middle channel in this simulation setup which was similar to the actual experimental situation. When generating submerged flow, different heights of tails at the end of the channel were set to control the depth of the channel. An outflow

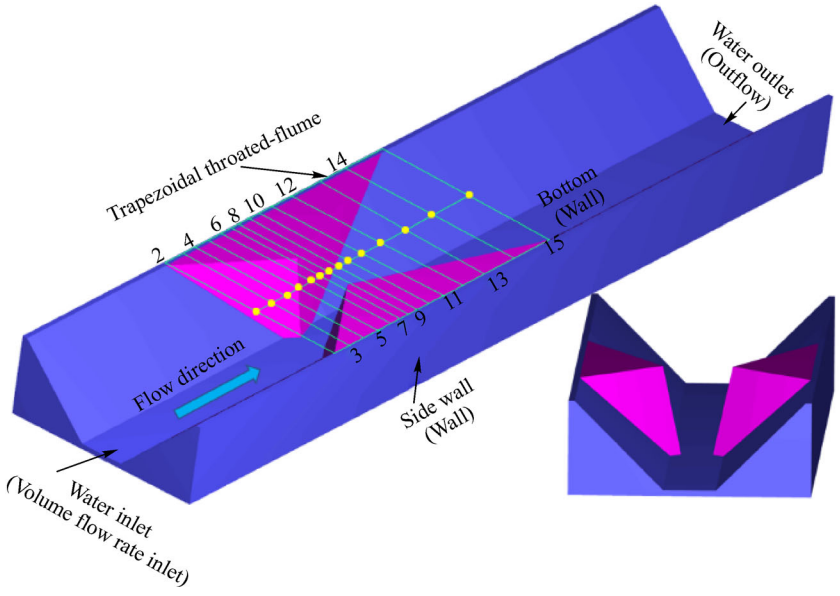

Fig. 3 Entire model geometry and boundary conditions

outlet condition was positioned on the downstream backwater drainage channel exit. The bottom of the model and the side walls were set as a wall boundary condition. Also, the air inlet at the top of the model was set as a symmetry boundary condition, where no fluid flowed through the boundary.

As shown in Fig. 3, We set 16 measuring cross-sections in laboratory experiments to measure hydraulic parameters of flow, numbered 1–16, two sections were upstream and downstream of the flume and the other 14 control sections were in the flume. Section1 was 2 m distant from the entrance of the flume, section 2 was the entrance section of the flume, and section 15 was exit the section of the flume, and section 16 was 2 m distant from the exit of the flume. The locations of the other sections are shown in Table 1.

4 Results and analysis

4.1 Model validation

Precise measurement of average velocity is essential for governing the total discharge in an open channel. Average velocity observed in the experiments with 12 working conditions coincided closely with estimations from the FLOW-3D model. Average velocity is the value calculated by the depth of each measuring cross section in the experiments. Both experimental and simulated average velocity at 34.77 $L \cdot s^{-1}$ are shown in Fig. 4. It is clear in Fig. 4 that average velocity rose as flow depth decreased under free flow conditions. In comparison, under submerged flow conditions, the average velocity increased at first, peaked at 0.12 m downstream from the throat, and decreased to the outlet. The difference between experimental and simulated values with free and submerged flow were −6.27% and −9.55% to the maximum, respectively. These values represent a satisfactory agreement between experimental and simulated results.

4.2 Velocity distributions in the throat section

Velocity distribution in the throat section with discharge of 34.77 $L \cdot s^{-1}$ under free flow condition is presented in Fig. 5. Velocity near the side walls was much smaller than in the middle section. This is because the viscosity near the walls cannot be ignored, there are grater velocity gradients, and the large frictional resistance. Overcoming resistance will drain part of the energy and the effect on velocity is very large, so the velocity near the walls is relatively low.

4.3 Water surface profiles

The flow pattern is described using water surface profiles measured along the centerline of the flume under free and submerged flow conditions (Fig. 6). Water flowed smoothly through the inlet of trapezoidal cutthroat flume and began to descend slowly near the throat. Owing to the lateral convergence of the throat, there was a sudden drop of water surface profile when the water depth reached a minimum value. Thus, the flow state changes from subcritical to supercritical. There were hydraulic jumps at the end of the outlet of the trapezoidal cutthroat flume under both free and submerged flow conditions. Finally, as the water was discharged through the outlet of the trapezoidal channel, the downstream water level began to rise slowly.

4.4 Discharge calculation formula

The constriction of the throat affects critical flow and has an important role in flow measurement. According to the correlations between discharges and depths at each upstream cross section in converging sections, the depth in the section 2 and discharge had the most solid correlation with a coefficient of 0.992. Thus, depth in section 2 was chosen to calculate discharge. An equation of upstream depth versus discharge with free flow is given by Eq. (8), and an equation of upstream depth and submergence ratio versus discharge with submerged flow is given by Eq. (9).

$$Q = 0.659h^{1.671} \tag{8}$$

$$Q = 1.416S\sqrt{1-S}H^{1.490} \tag{9}$$

Table 1 The position of each control section

Section number	Length from section 1/m	Section number	Length from section 1/m
1 (Upstream)	0.00	9	2.90
2 (Inlet of the flume)	2.00	10	2.95
3	2.35	11	3.05
4	2.55	12	3.15
5	2.65	13	3.25
6	2.75	14	3.45
7	2.80	15 (Outlet of the flume)	4.55
8 (Throat section)	2.85	16 (Downstream)	6.55

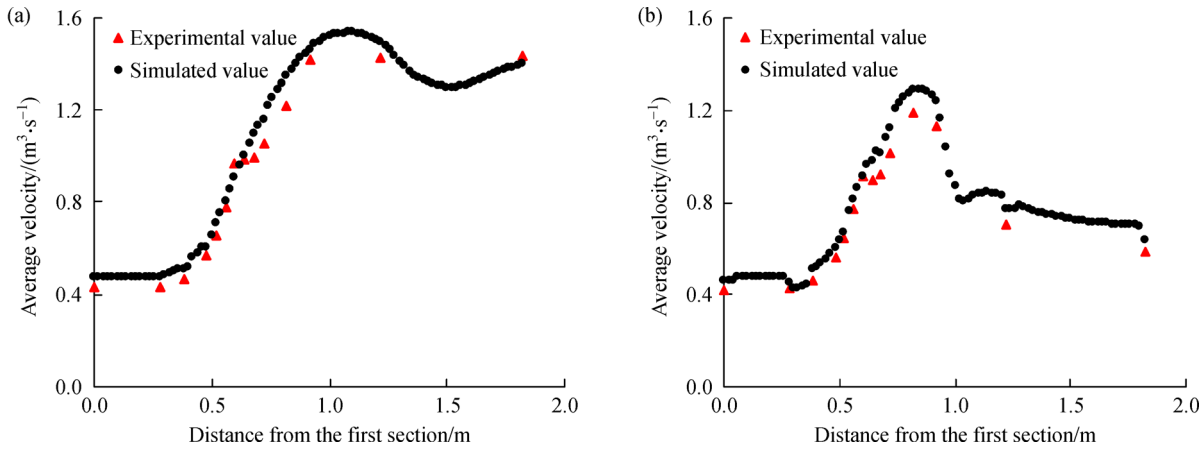

Fig. 4 Average velocity variation along the flow of trapezoidal cutthroat flume. (a) Free flow; (b) submerged flow.

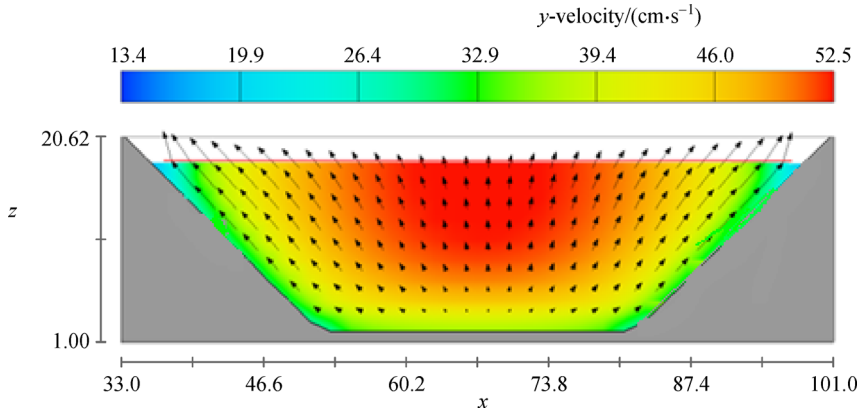

Fig. 5 Velocity distribution in the throat section with discharge of 34.77 L·s^{-1} under free flow condition

To validate Eqs. (6)–(7), the calculated results and the measured discharges are compared in Table 2. The measured and calculated discharge values are in reasonable agreement with ±5% errors. In addition, the maximum errors of calculated discharge using the depth-discharge equation with free and submerged flow were 1.88% and −2.62%, respectively, which met the standard requirement for accuracy of irrigation systems.

4.5 Distribution of Froude number

Froude number is a dimensionless parameter used to discriminate flow regimes[30]. Flow is considered subcritical when the Froude number is less than 1; supercritical when the Froude number is greater than 1; and critical when the Froude number is 1[10]. The Froude number along the center line of the flume predicted by FLOW-3D software are shown in Fig. 7. Under free flow conditions, the Froude number increased at the converging section, and kept increasing near the downstream end of the throat. Then, the Froude number peaked in the front part of the diffusion section. Finally, the Froude number decreased rapidly. At the converging section, the Froude numbers were less than 0.5, and increased to 1 near the throat, then decreased to less than one. Near the throat, the state of flow changed from subcritical to supercritical, which met the requirement of the Froude number in flow measurement. The change law of Froude number under submerged outflow condition was the same as that of free flow conditions.

4.6 Analysis of the head loss

Trapezoidal cutthroat flumes are characterized by the shape of the trapezoidal cross-sectional area. The shape aims to contract the width of the original channel in order to ensure that the critical depth occurs in the narrow section, although it brings some head loss. A comparison between the head loss caused by the trapezoidal cutthroat flume and a rectangular cutthroat flume was made. The head loss of the flume was defined as the difference between the head in a section 2 m upstream of the flume entrance and the head

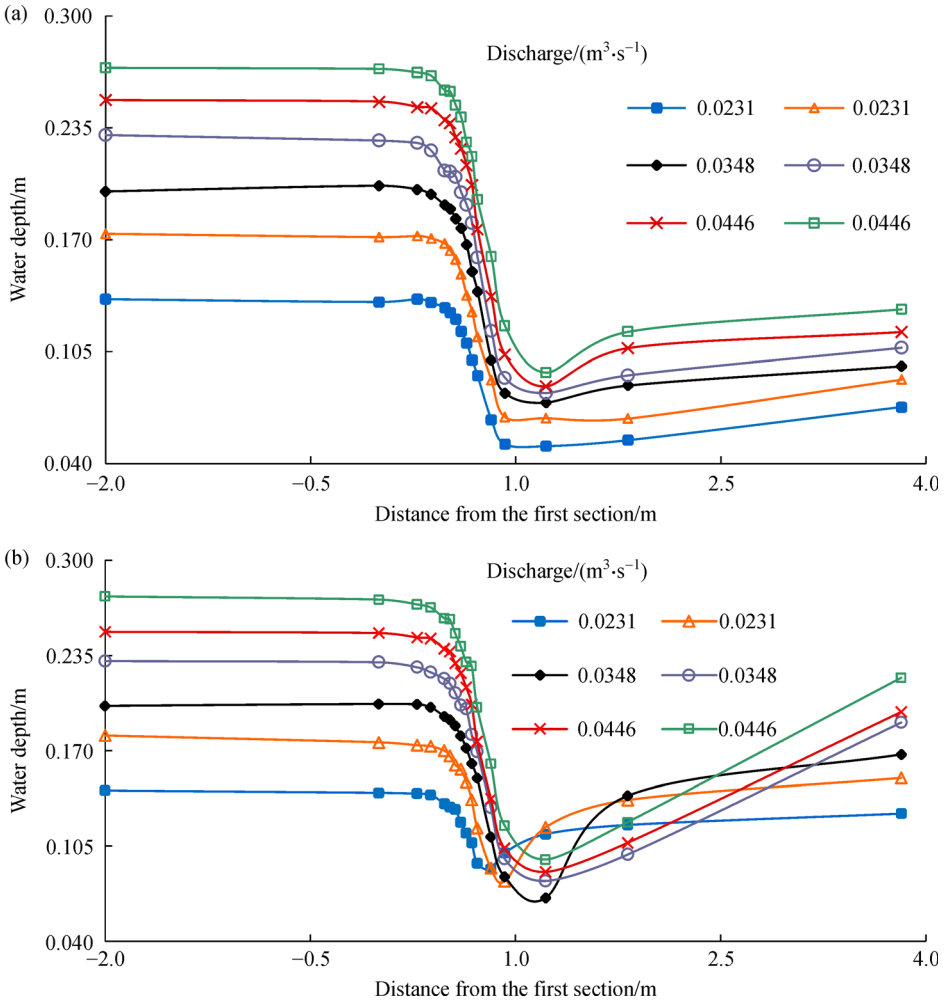

Fig. 6 Variation of the water surface profiles along the centerline of the flume. (a) Free flow; (b) submerged flow.

Table 2 Calculation errors for trapezoidal cutthroat flume under different conditions

Outflow condition	Practical discharge/($m^3 \cdot s^{-1}$)	Depth in the first section of the throat	Calculated discharge/($m^3 \cdot s^{-1}$)	Relative error/%
Free flow	0.02308	0.1339	0.02289	0.80
	0.03477	0.1716	0.03465	0.33
	0.04462	0.2014	0.04529	−1.49
	0.05500	0.2277	0.05560	−1.08
	0.06500	0.2503	0.06512	−0.18
	0.07500	0.2693	0.07359	1.88
Submerged flow	0.02308	0.1413	0.02263	1.93
	0.03477	0.1756	0.03568	−2.62
	0.04462	0.2019	0.04435	0.59
	0.05500	0.2305	0.05549	−0.89
	0.06500	0.2503	0.06563	−0.97
	0.07500	0.2731	0.07339	2.14

in a section 2 m downstream of the flume exit. The head included water level head, pressure head and velocity head. The head losses were calculated by using Eq. (10).

$$h_f = (Z_a + P_a/\gamma + V_a^2/2g) - (Z_b + P_b/\gamma + V_b^2/2g) \quad (10)$$

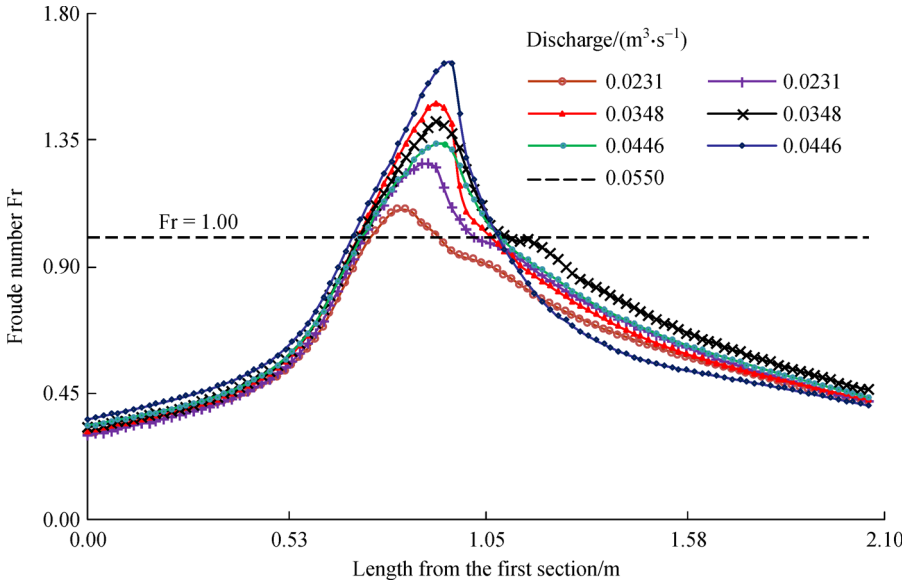

Fig. 7 Development of Froude number along flume under different discharge conditions

The head losses caused by the trapezoidal cutthroat flume and the rectangular cutthroat flume are given in Table 3. Under free flow conditions, the head losses were increased while discharge rose, but when the discharge was more than 0.045 $m^3 \cdot s^{-1}$, the head loss increased, but more slowly where there was a hydraulic jump. The head losses caused by a trapezoidal cutthroat flume was less than the head losses caused by rectangular cutthroat flume under the same discharge conditions. However, the head loss of the trapezoidal cutthroat flume under free flow conditions, due to excluding the energy consumed by hydraulic jumps downstream of flume exit, was more than that under submerged flow conditions.

Table 3 Head losses of trapezoidal and rectangular cutthroat flumes under different discharges when the throat constriction rate is 0.506

Discharge/($m^3 \cdot s^{-1}$)	Head loss of rectangular throat/%	Head loss of trapezoidal throat/%
0.0154	3.139	2.350
0.0194	3.352	3.110
0.0231	3.733	3.450
0.0294	4.143	3.890
0.0348	5.613	5.110
0.0392	5.921	5.160
0.0446	6.258	6.110
0.0496	7.192	6.980
0.0550	7.367	6.990
0.0612	9.822	7.890
0.0650	10.566	8.335
0.0750	11.097	8.955

5 Conclusions

In this study, three-dimensional flow fields in a trapezoidal cutthroat flume were simulated using the turbulence model RNG k-ε along with the TruVOF method. Comparison of experimental and computated results of the velocity and the water profiles shows that the TruVOF method can capture the free surface of open channel flow and simulate the flume flow process accurately.

The velocity distribution and Froude number for a trapezoidal cutthroat flume were analyzed. It was found that the velocities near the walls are much lower than in the middle section. The Froude number was less than 0.5 at the converging section, and the state of flow changed from subcritical to supercritical near the throat, which met the requirements of the Froude number in flow measurement. By analysis and derivation, equations of upstream depth versus discharge under free and submerged flow conditions were fitted by regression analyses with a deviation of $\pm 5\%$, which meets the requirement of flow measurement with discharges of up to 0.075 $m^3 \cdot s^{-1}$ in irrigation systems. Additionally, the head loss caused by the trapezoidal cutthroat flume and rectangular cutthroat flume were calculated. It was found that a trapezoidal cutthroat flume installed in trapezoidal channel had a smaller head loss. All in all, it is concluded that trapezoidal cutthroat flume has the advantages of simple structure, low cost, small head loss and high accuracy, plus it can be applied to different water resource conditions, especially when there is excessive sediment. Trapezoidal cutthroat flumes are more suitable for flow measurement in a trapezoidal channel owing to that improved measurement accuracy while sacrificing less water head.

Acknowledgements The authors would like to acknowledge the financial support given by the Special Fund for Agro-scientific Research in the Public Interest of China (201503125) and the National Key Research and Development Program of China (2016YFC0400200).

Compliance with ethics guidelines Danjie Ran, Wene Wang, and Xiaotao Hu declare that they have no conflicts of interest or financial conflicts to disclose.

This article does not contain any studies with human or animal subjects performed by any of the authors.

References

1. Galán-Martín A, Vaskan P, Vallejo A, Esteller L J, Guillén-Gosálbez G. Multi-objective optimization of rainfed and irrigated agricultural areas considering production and environmental criteria: a case study of wheat production in Spain. *Journal of Cleaner Production*, 2017, **140**(2): 816–830
2. Wang Y B, Liu D, Cao X C. Agricultural water rights trading and virtual water export compensation coupling model: a case study of an irrigation district in China. *Agricultural Water Management*, 2017, **180**(Part A): 99–106
3. Valipour M. Increasing irrigation efficiency by management strategies: cutback and surge irrigation. *Journal of Agricultural and Biological Science*, 2013, **8**(1): 35–43
4. Wang C D. Water measurement technique and measure. Beijing: *Water and Power Press*, 2005 (in Chinese)
5. Samani Z, Magallanez H. Closure to "Simple flume for flow measurement in open channel" by Zohrab Samani and Henry Magallanez. *Journal of Irrigation and Drainage Engineering*, 2002, **128**(2): 129–131
6. Cone V M. The Venturi flume. *Journal of Agricultural Research*, 1917, **6**(4): 115–129
7. Parshall R L. The improved Venturi flume. *Transactions of the American Society of Civil Engineers*, 1926, **89**(1): 841–851
8. Skogerboe G V, Hyatt M L. Rectangular cutthroat flow measuring flumes. *Proceedings of the American Society of Civil Engineers*, 1967, **93**(IR4): 1–13
9. Clemmens A J, Bos M G, Replogle J A. RBC broad-crested weirs for circular sewers and pipes. *Journal of Hydrology*, 1984, **68**(1–4): 349–368
10. Lv H X, Pei G X, Yang L X. Hydraulics. Beijing: *Agriculture Press*, 2011 (in Chinese)
11. Parshall R L. Parshall measuring flume. *Colorado Experiment Station Bulletin*, 1936, 423
12. Hager W H. Modified Venturi channel. *Journal of Irrigation and Drainage Engineering*, 1985, **111**(1): 19–35
13. Jesson M, Sterling M, Baker D. Application of ISO4359 for discharge calculation in a narrow flume. *Flow Measurement and Instrumentation*, 2017, **54**: 283–287
14. Das R, Nayek M, Das S, Dutta P, Mazumdar A. Design and analysis of 0.127 m (5″) cutthroat flume. *Ain Shams Engineering Journal*, 2017, **8**(3): 295–303
15. Mazumdar A, Dutta P, Nayek M. Calibration and Discharge Measurement Using 0.127 Meter (5″) Parshall Flume. *Iahr World Congress*, 2017
16. Jing S Y, Wang L, Du H, Wei G. Applications of FLOW-3D in numerical simulation of fluid-structure interaction. *The 13th National Hydrodynamic Academic Conference and the Twenty-Sixth National Hydrodynamics Seminar*, 2017, 423–428
17. FLOW-3D® User Manual. FLOW-3D User Manual. *Flow Science*, 2016
18. Yakhot V, Orszag S A. Renormalization group analysis of turbulence I. Basic theory. *Plenum Press*, 1986
19. Xiao Y, Zhang J B, Yao B, Guan Y. Assembly and simulation analysis of shear-sheet machine based on Pro/E. *Procedia Engineering*, 2011, **16**(1): 535–539
20. Bayon A, Toro J P, Bombardelli F A, Matos J, López-Jiménez P A. Influence of VOF technique, turbulence model and discretization scheme on the numerical simulation of the non-aerated, skimming flow in stepped spillways. *Journal of Hydro-environment Research*, 2017. doi: 10.1016/j.jher.2017.10.002
21. Wan B L, He W X, Chen C Y. Assembly process bill of material construction technology for dpacecraft assembly and integration based on proengineer. *Joint International Information Technology, Mechanical and Electronic Engineering Conference*, 2017
22. Pan Z B, Lü H X, Zhang X F. Experiment on airfoil-shaped measuring flume in trapezoidal canal. *Transactions of The Chinese Society of Agricultural Machinery*, 2009, **40**(12): 97–100 (in Chinese)
23. Najafi-Jilani A, Niri M Z, Naderi N. Simulating three-dimensional wave run-up over breakwaters covered by antifer units. *International Journal of Naval Architecture and Ocean Engineering*, 2014, **6**(2): 297–306
24. Duguay J M, Lacey R W J, Gaucher J. A case study of a pool and weir fishway modeled with open foam and FLOW-3D. *Ecological Engineering*, 2017, **103**: 31–42
25. Cui W, Song H F. CFD simulation of fresh self-compacting concrete flow and casting process. *Concrete*, 2017, **1**(8): 111–115
26. Xiao Y Z, Wang W N, Hu X, Zhou Y. Experimental and numerical research on portable short-throat flume in the field. *Flow Measurement and Instrumentation*, 2016, **47**: 54–61
27. Tekade S A, Vasudeo A D, Ghare A D, Ingle R N. Measurement of flow in supercritical flow regime using cutthroat flumes. *Sādhanā*, 2016, **41**(2):265–272.
28. Samani Z. Three simple flumes for flow measurement in open channels. *Journal of Irrigation & Drainage Engineering*, 2017, doi: org/10.1061/(ASCE)IR.1943-4774.0001168
29. Hu H, Huang J, Qian Z, Yu G. Hydraulic analysis of parabolic flume for flow measurement. *Flow Measurement and Instrumentation*, 2014, **37**: 54–64
30. Zhang L, Wu P T, Zhu D L, Zheng C. Flow regime and head loss in a drip emitter equipped with a labyrinth channel. *Journal of Hydrodynamics*, 2016, **28**(4): 610–616